



Research Paper

XY SCANNING MECHANISM: A DYNAMIC APPROACH

Sollapur Shrishail B¹* and Deshmukh Suhas P¹

*Corresponding Author: Sollapur Shrishail B, ✉ shrishail.sollapur@gmail.com

Flexure mechanisms have immense scope in their use for applications involving high precision motion. There are many concepts to build high speed or high precision manipulators, but only a few of them can serve to obtain high speed together with high precision. Mathematical modeling of simple XY manipulator is carried out XY manipulator uses typical Double Flexural configurations. Static and dynamic analysis is carried out using MATLAB. Static analysis is carried out to determine static deflection of motion stage with force. It is observed that force deflection curve is linear. Dynamic analysis is carried out to determine frequencies and mode shapes of flexural manipulator. Further, Finite Element software ANSYS is used to carry out static and dynamic analysis of basic DFM configuration and few XY mechanisms. It is observed that close matching of FEM results with model developed.

Keywords: Flexural mechanism, FEA analysis

INTRODUCTION

Several publications talk about the pros and cons of flexure mechanisms and highlight the significance of their use in technology required to provide energy efficient, wear free, higher resolution and high speed devices. Flexures have been used as bearings to provide smooth and guided motion, for example in precision motion stages; as springs to provide preload, for example in the brushes of a DC motor or a camera lens cap; to avoid over-constraint, as in the case of bellows or helical

coupling; as clamping devices, for example, the collet of a lathe, for elastic averaging as in a windshield wiper, and for energy storage, such as, in a bow or a catapult. This list encompasses applications related to the transmission of force, displacement as well as energy, thereby making the versatility of flexures quite evident.

A historical background of flexures is presented in several texts. Flexure design is traditionally based on creative thinking and engineering intuition, analytical tools can aid

¹ Department of Mechanical Engineering, Sinhgad Academy of Engineering, Pune, India.

the design conception, evaluation and optimization process. Consequently, a systematic study and modeling of these devices has been an active area of research. Some of the existing literature deals with precision mechanisms that use flexures as replacements for conventional hinges, thus eliminating friction and backlash. Analysis and synthesis of these mechanisms is simply an extension of the theory that has already been developed for rigid link mechanisms, except that in this case the range of motion is typically small. The key aspect of these mechanisms is flexure hinge design. Unlike these cases where compliance in the system is limited to the hinges, other flexure mechanisms exist in which compliance is distributed over a larger part of the entire topology. Both these kinds of mechanisms offer a rich mine of innovative and elegant design solutions for a wide range of applications.

Any systematic flexure design exercise has to be based on performance measures. While detailed performance measures can be laid out depending on specific applications, a general set of measures are highlighted here. These measures are based on the deviation of flexures from ideal constraints.

One of the primary applications of flexures is in the design of motion stages. This thesis strives to bridge the gap between intuition and mathematical analysis in flexure mechanism design. Accordingly, the following list highlights the specific contributions of this thesis.

1. Dynamic Modeling of double flexural manipulator is carried to determine its natural modes and mode shapes using assumed modes method.

2. Modal analysis and frequency response is determined for DFM considering actuator dynamics.
3. Static analysis is carried for DFM.
4. FEM analysis of DFM is carried out and comparison of results of assumed modes method and ANSYS results is done.

High precision measuring technologies such as the Scanning Probe Microscope (SPM), Atomic Force Microscope (AFM), electron microscope, X-ray microscope, and confocal scanning microscope are rapidly advancing via the development of semiconductor processing technologies and biomedical technologies. Most of these microscopes require a precise multi-axis scanner for sample scanning, and many scanners with nanometer-level resolution have been developed.

The majority of practical nano-positioners utilize flexure-based structures, such as compliant mechanisms and notch-flexure-based mechanisms, due to their smooth and friction-free motion and high durability without wear and deterioration. Piezoelectric actuators and high resolution displacement sensors are widely used with flexure-based mechanisms to obtain displacement with nanometer level resolution. Among the flexure-based mechanisms, parallelogram mechanisms restrict all rotational degrees-of-freedom of the connector (end-effector) and keep the connector parallel to the base, because of the equal lengths for its crank and followers (the members connected to the base). In spite of rotation of the crank and the follower, the connector undergoes pure translation along a circular path. Due to this feature, parallelogram

mechanisms can be directly used as single degree-of-freedom nano-positioning modules. Such nano-positioning modules can be easily configured as building blocks to build a multi-degree-of-freedom nano-positioner. Parallelogram mechanisms have also been used in many other applications, such as delta-robots and other low degree-of-freedom parallel kinematics nano-positioning stages.

Compliant mechanisms transmit motion and force by deflection of their flexible members. They are usually made of a monolithic piece of material and thus involve no wear, backlash, noise, and lubrication. To predict more accurately their deflected shape in larger working range, the analysis of compliant mechanisms has usually based on nonlinear numerical techniques such as the finite element method. To increase the working range of a compliant mechanism, its members usually undergo large displacement and rotation. Unlike structural members whose deflection is small so that the linear beam theory holds, compliant members capable of large displacement and rotation require a nonlinear analysis to accurately predict their deformed configuration. Some commonly used nonlinear analytical methods include the elliptical integrals, the chain algorithm, and the Finite Element Method (FEM). Since positioning systems play a crucial role in many nanotechnology applications, they have attracted considerable interest from many scholars and research bodies in recent years. A review of the available literature reveals that positioning devices can broadly be divided into three categories in terms of the particular method utilized to drive the stage. These categories are: (1) stick-slip induced friction

drive stages, (2) clamp release inchworm-screw stages and (3) elastic deformation stages.

Assumed Modes Method: Double Parallelogram Flexure Mechanism:

Using the assumed modes technique, we would first find the natural frequencies and mode shapes of the X-stage and later use these to arrive at the dynamic equations of this system.

From the Euler-Bernoulli beam theory, each beam satisfies

$$\frac{\partial^2}{\partial x^2} \left[EI \frac{\partial^2 y}{\partial x^2} \right] = - \frac{m \partial^2 y}{\partial t^2} \quad \dots(1)$$

By separation of variables:

$$y(x, t) = Y(x)F(t) \quad \dots(2)$$

Assuming a harmonic form (conserving the total energy of a conservative system) for the time dependent component:

$$\frac{d^4}{dx^4} EI Y(x) = \check{S} m Y(x) \quad \dots(3)$$

Since 'EI' is independent of x and t

$$\frac{d^4 Y}{dx^4} - b^4 Y = 0; b^4 = \frac{\check{S}^2 m}{EI} \quad \dots(4)$$

Equation gives us the beam mode shapes Y corresponding to each natural frequency \check{S} . The general solution (for the i^{th} beam) to this problem is of the form:

$$Y(x) = C_{i1} \sin bx + C_{i2} \cos bx + C_{i3} \sin hbx + C_{i4} \cos h \quad \dots(5)$$

By symmetry, the two beams in the upper half will have the same mode shapes as their corresponding counterparts in the lower half. We therefore analyze the boundary conditions

for beam 1 and beam 2 as depicted in fig for the case of free vibrations.

Boundary Conditions (subscript represents the beam number):

$$Y_1|_{x=0} = Y_2|_{x=0}, \frac{dY_1}{dx}|_{x=0} = \frac{dY_2}{dx}|_{x=0} \quad \dots(6)$$

$$Y_1|_{x=L} = 0, \frac{dY_1}{dx}|_{x=L} = 0, \frac{dY_2}{dx}|_{x=L} = 0$$

$$\frac{d^3Y_2}{dx^3}|_{x=L} = -\frac{Mp}{2m}b^4Y_2|_{x=L}$$

$$\frac{d^3Y_1}{dx^3}|_{x=0} + \frac{d^3Y_2}{dx^3}|_{x=0} = \frac{M_1}{2m}b^4Y_{1or2}|_{x=0} \quad \dots(7)$$

The above boundary conditions give us eight equations in the nine unknowns and solving these boundary condition we get:

$$c_{21} \left(-\cos bL - \cosh bL + \frac{M_p}{2m}b \sin bL - \frac{M_p}{2m}b \sin hbL \right) + c_{22} \left(\sin bL + \frac{M_p}{2m}b \cos bL \right) + c_{24} \left(\sin bL + \frac{M_p}{2m}b \cos hbL \right) = 0 \quad \dots(8)$$

$$-c_{21} - \frac{M_1}{2m}bc_{12} + c_{13} - \frac{M_1}{2m}bc_{14} - c_{21} + c_{23} = 0 \quad \dots(9)$$

Using matrix notation, they take the form's $(b) = 0$. These equations were then solved using an optimization algorithm to find the values of the unknowns.

Using Values Specific to Our Setup

Mass of primary motion stage (M_p) = 0.307 kg

Mass of secondary/intermediate motion stage (M) = 0.070 kg

Beam material density: 7860 kg per cubic metre

Beam thickness = 0.05 cm

Mass/ unit length (m) = 0.09825 kg/m

Beam Length (L) = 12.5 cm

Width = 2.5 cm

Area of cross section of beam = $1.25 \times 10^{-5} \text{ m}^2$

Young's Modulus (E) = $1.131 \times 10^{11} \text{ pa}$

Results show that the final transfer function depends primarily on the first two modes of the system. The contribution from the remaining modes is not very significant. Hence, using only the first two modes:

Mode Shapes

Frequency: 3.93 Hz

$$Y_1(x) = 0.237 \sin bx - 0.108 \cos bx - 0.237 \sinh bx + 0.086 \cosh bx$$

$$Y_2(x) = -0.213 \sin bx + 0.074 \cos bx - 0.213 \sinh bx - 0.095 \cosh bx$$

Frequency: 16.13 Hz

$$Y_1(x) = 0.237 \sin bx - 0.108 \cos bx - 0.237 \sinh bx + 0.086 \cosh bx$$

$$Y_2(x) = 0.053 \sin bx - 0.071 \cos bx - 0.053 \sinh bx + 0.03 \cosh bx$$

The value $Y_i(x)$ can be scaled using a normalizing constant. It can be easily verified that this constant has no effect on the final system transfer function obtained using these modeshapes. The modeshapes are shown in Figures 2 and 4.

Figure 1: Frequency 3.93 Hz via AMM

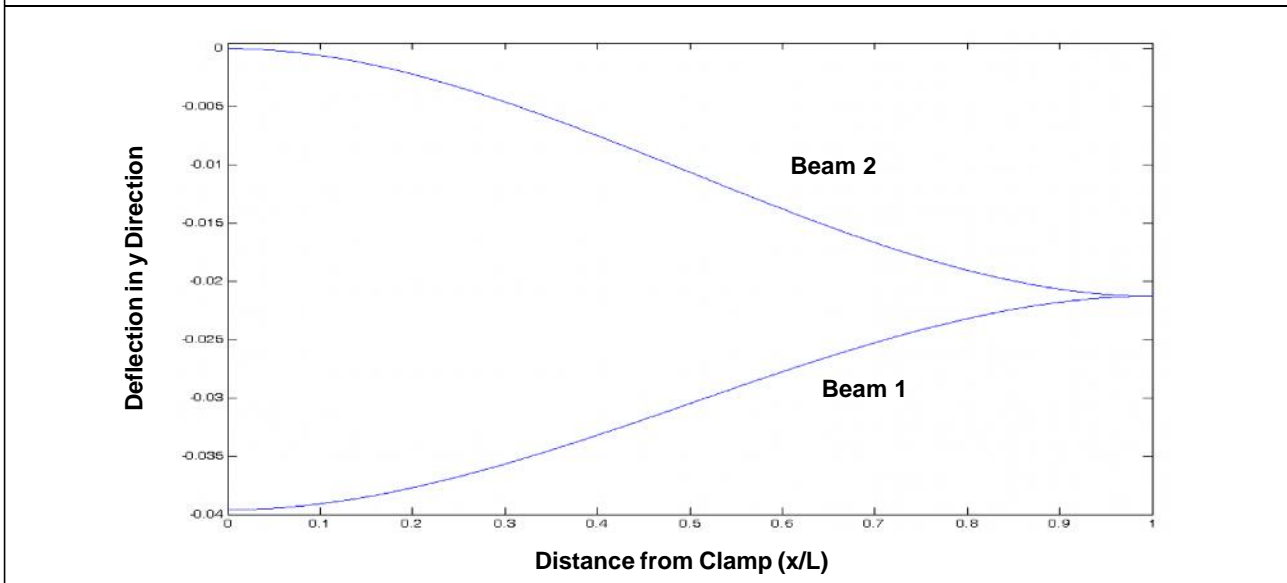


Figure 2: Mode Shape 1: Frequency 4.03 Hz via FEM (Ansys)

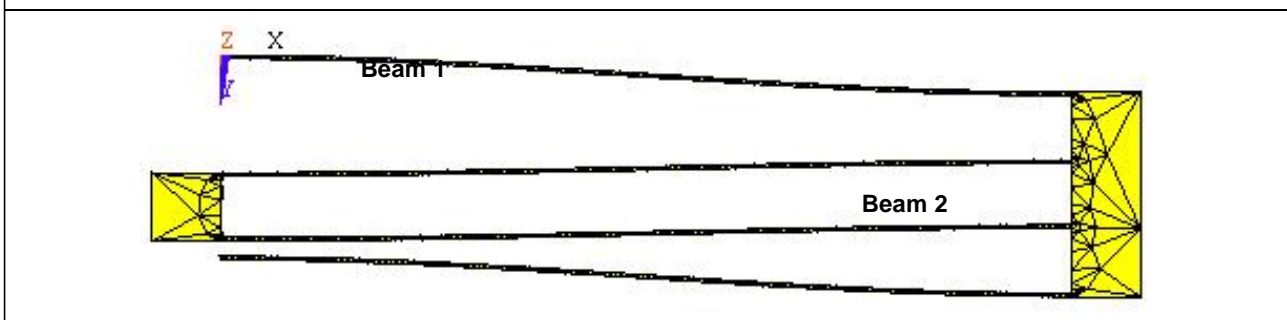


Figure 3: Frequency 16.13 Hz via AMM

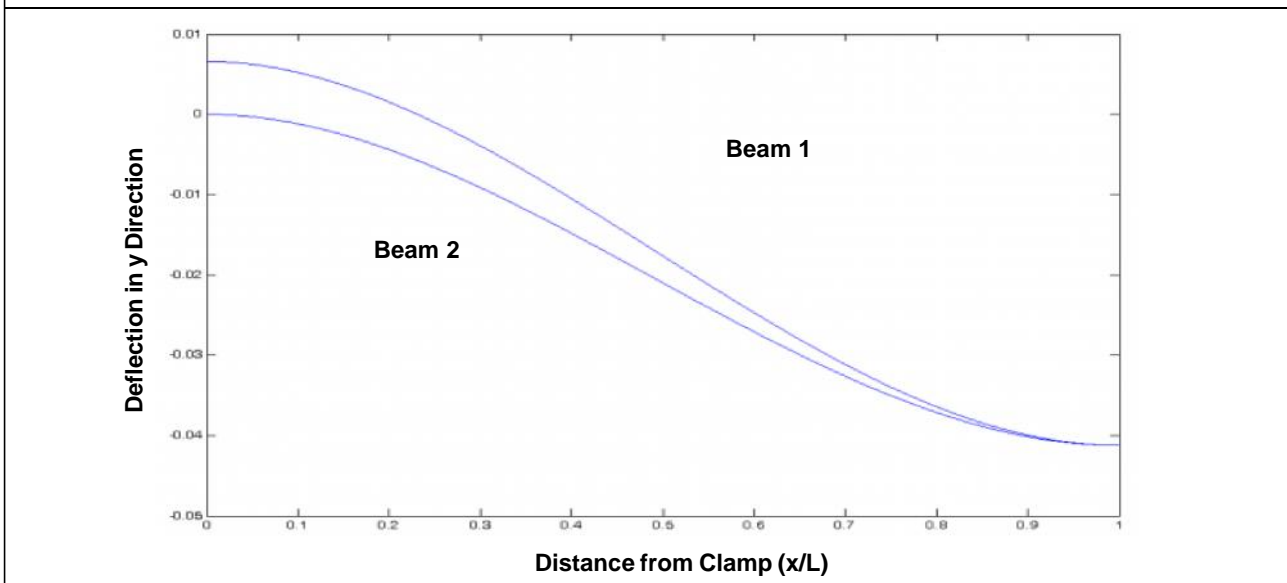
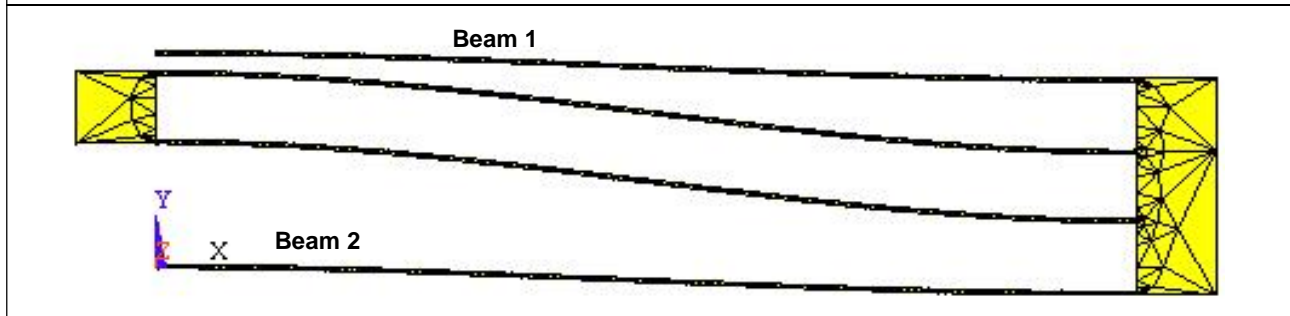


Figure 4: Mode Shape 2: Frequency 16.63 Hz via FEM (Ansys)



Since the two beams will move together in the presence of any frequency excitation, the generalized time coordinate $q_i(t)$ for these will be the same; the mode shapes will differ. From the assumed modes method theory and using only mode 1 and 2, displacement 'y' for each beam in its own frame can be expressed as:

$$y = \sum_{i=1}^n w_i(x)q_i(t), n = 2$$

For the case above, the energy equations for the system are:

$$K(t) = 2 \times \left(\frac{1}{2} \int_0^L m \left[\frac{\partial y(x,t)}{\partial t} \right]^2 dx \right)_{beam1} + 2 \times \left(\frac{1}{2} \int_0^L m \left[\frac{\partial y(x,t)}{\partial t} \right]^2 dx \right)_{beam2} + \frac{1}{2} M_p \left[\frac{\partial y(L,t)}{\partial t} \right]^2 + \frac{1}{2} M_l \left[\frac{\partial y(0,t)}{\partial t} \right]^2 \quad \dots(10)$$

$$V(t) = 2 \times \left(\frac{1}{2} \int_0^L EI \left[\frac{\partial^2 y(x,t)}{\partial x^2} \right]^2 dx \right)_{beam1} + 2 \times \left(\frac{1}{2} \int_0^L EI \left[\frac{\partial^2 y(x,t)}{\partial x^2} \right]^2 dx \right)_{beam2} \quad \dots(11)$$

The kinetic energy can be written as:

$$K(t) = \sum_{i=1}^n \sum_{j=1}^n m_{ij} \dot{q}_i(t) \dot{q}_j(t) \quad \dots(12)$$

The potential energy can be written as:

$$V(t) = \sum_{i=1}^n \sum_{j=1}^n k_{ij} q_i(t) q_j(t) \quad \dots(13)$$

Using Lagrange equation with $L = K - V$;

$$\frac{\partial L}{\partial q} - \frac{d}{dt} \left(\frac{\partial L}{\partial \dot{q}} \right) = 0$$

This gives the equation of motion for free vibration:

$$[M] \{\ddot{q}\} + [K] \{q\} = 0 \quad \dots(14)$$

For our case

$$M = \begin{pmatrix} 2.6 \times 10^{-4} & 0 \\ 0 & 1 \times 10^{-4} \end{pmatrix}$$

$$K = \begin{pmatrix} 0.1475 & 0 \\ 0 & 1.0278 \end{pmatrix}, F = \begin{pmatrix} -0.0375 \\ 0.0068 \end{pmatrix}$$

State Space Form

Choosing $q_1, \dot{q}_1, q_2, \dot{q}_2$ as the state variables, the equations can be written in the form

where

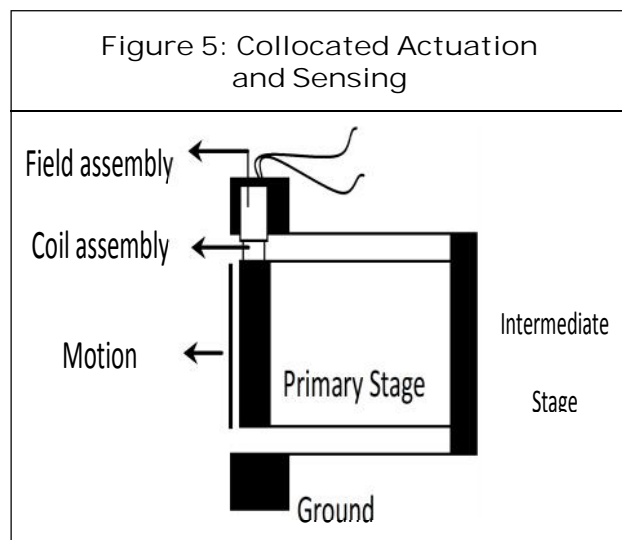
$$x = \begin{pmatrix} q_1 \\ \dot{q}_1 \\ q_2 \\ \dot{q}_2 \end{pmatrix}$$

and A, B, C are matrices given by:

$$A = \begin{pmatrix} 0 - 0.7 \times 10^{-4} & 0 - 5.8 \times 10^6 \\ 1 & 0 & 0 & 0 \\ 0 & 1 & 0 & 0 \\ 0 & 0 & 1 & 0 \end{pmatrix}$$

$$B = \begin{pmatrix} 1 \\ 0 \\ 0 \\ 0 \end{pmatrix}, C = (0 \quad 58.67 \quad 0 \quad 5.55 \times 10^5)$$

Coupled Equations: Flexural Mechanism and Linear Voice Coil Actuator

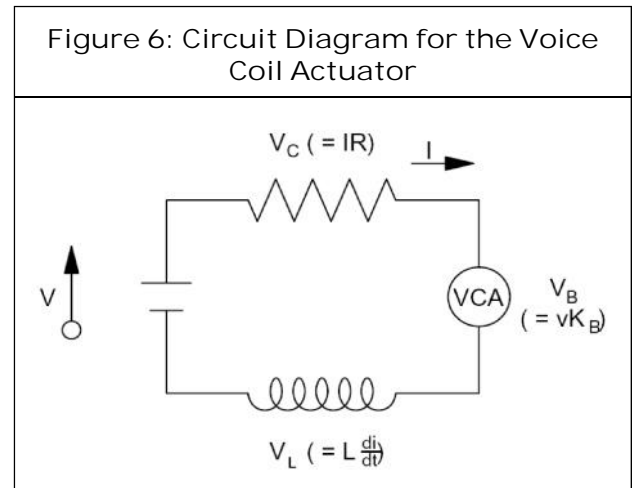


The mechanism is actuated using a Linear Voice Coil Actuator (shown above). In the final assembly, the coil assembly mass of the voice coil actuator is attached to and moves with the primary motion stage. Thus, in the equation the effective mass of the primary stage changes to mass (primary stage) + mass (coil assembly).

Equations: Voice Coil Actuator

The voltage drop across the actuator can be written as $V(t) = V(t)_{resistance} + V(t)_{backemf} + V(t)_{inductance}$

The values specific to our actuator model are:



Force sensitivity (K_f) = 5.78 N / Amp

Back EMF constant (K_b) = 5.77 V / msec

Resistance (R) = 4.4 Ohm

Inductance (L) = 1.4e-3 Henry

Mass of the coil assembly (M_{ca}) = 0.0249 Kg

The value of inductance is very low and as such it affects the transfer function of the system only at high frequencies (>800 rad/s). Hence, neglecting inductance and coupling the above equation with the double parallelogram equation, we get:

$$\dot{x}(t) = A_{vc} x(t) + B_{vc} V(t), y(t) = C_{vc} x(t)$$

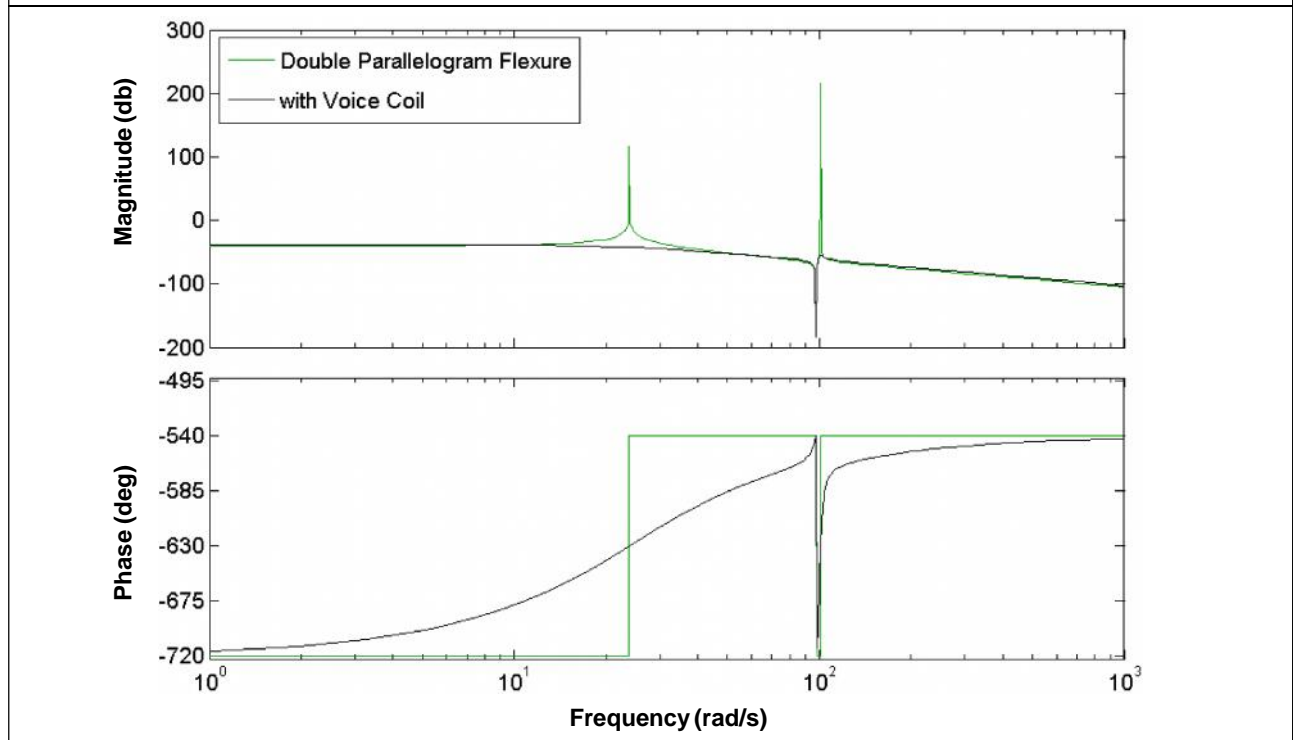
where

$$A_{vc} = A + \frac{K_f K_b}{R} B, B_{vc} = \frac{K_f}{R} B, C_{vc} = C$$

$$A = \begin{pmatrix} 0 - 0.7 \times 10^{-4} & 0 - 5.8 \times 10^6 \\ 1 & 0 & 0 & 0 \\ 0 & 1 & 0 & 0 \\ 0 & 0 & 1 & 0 \end{pmatrix}$$

$$B = \begin{pmatrix} 1.3136 \\ 0 \\ 0 \\ 0 \end{pmatrix}, C = (0 \quad 58.67 \quad 0 \quad 5.55 \times 10^5)$$

Figure 7: Bode Plots of Theoretically Derived Models: 1) Double Parallelogram Flexural Mechanism, and 2) The Overall Assembly, Including the Voice Coil

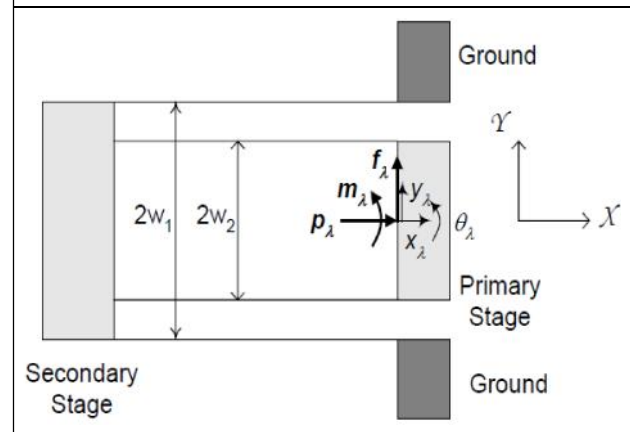


The voice coil back emf acts as a resistance and reduces bode plot amplitude in the lower frequency zone. The inductance has a similar effect over the higher frequency range.

Static and Dynamic Analysis of DFM
 Static Analysis of Flexural Mechanism

This flexure unit is also referred to as a compound parallelogram flexure, folded beam flexure or crab-leg flexure. Analysis shows that this flexure allows relative Y translation between bodies A and B, but is stiff in relative X displacement and rotation. The parasitic error along X direction, is considerably smaller because any length contraction due to beam deformation is absorbed by a secondary motion stage. There does exist a rotational parasitic motion, which may be eliminated by appropriate location of the Y direction force.

Figure 8: Double Flexure Mechanism



Hence, body A exhibits perfect Y-translation with respect to body B on the application of a Y direction force. These statements are true only in the absence of X direction forces.

The double parallelogram may be employed to construct XY mechanisms as shown in Figure. In these cases, cross axis coupling and

motion stage yaw should be small and actuator isolation should also be better than previous designs.

Beam material density = 7860 kg per cubic metre

Beam thickness = 0.05 cm

..... m) = 0.09825 kg/m

$$u = \frac{FL^3}{12EI}, \nu = t^2 \left[\frac{1}{b_1^2} + \frac{1}{b_2^2} \right] \frac{u}{L}, \nu = 0$$

Beam length (L) = 12.5 cm

Width = 2.5 cm

Area of cross section of beam = 1.23 x 10⁻⁵ m²

Young's modulus (E) = 1.31 x 10¹¹ pa

Figure 9: Comparison of Analytical and FEM-ANSYS Results for Static Analysis

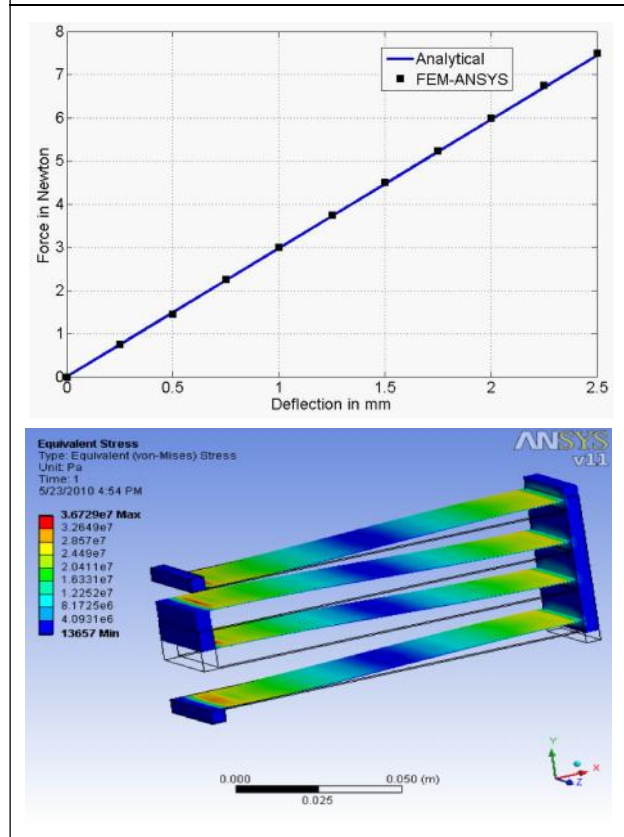


Figure 10: Static Analysis: Finite Element Results by Application of 1 N Load at Motion Stage

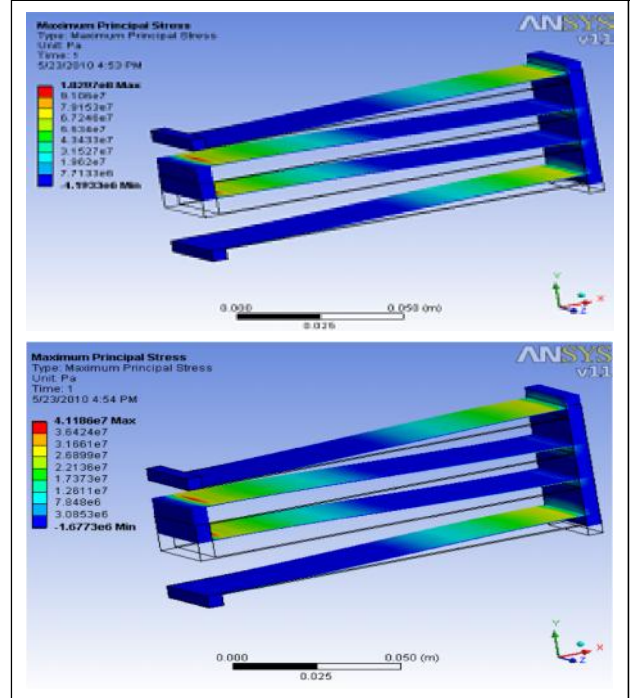


Figure 11: Static Analysis: Finite Element Results by Application of 2 N Load at Motion Stage

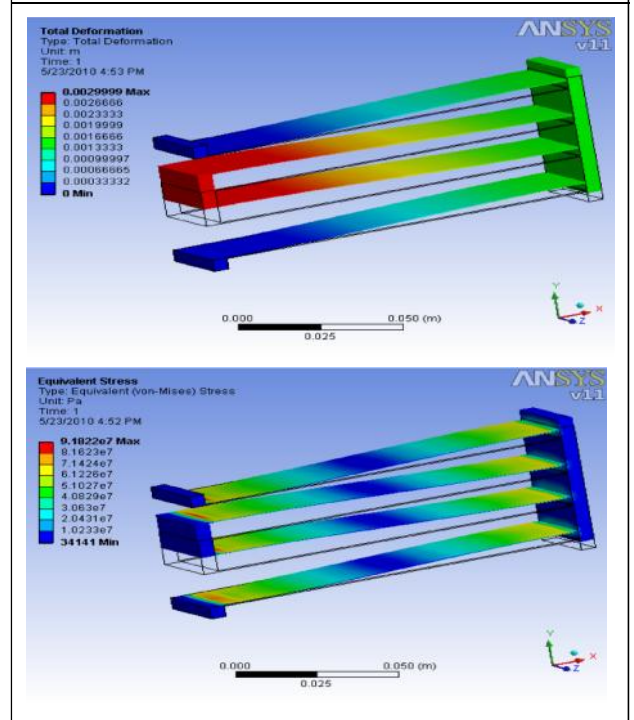
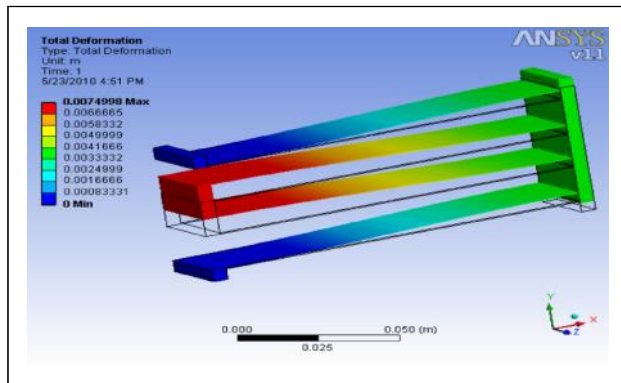


Figure 11 (Cont.)



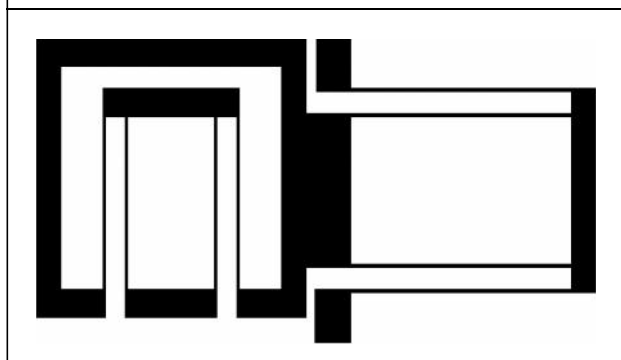
Deflection, angle of rotation and parasitic motion for double parallelogram flexural unit is given by following relations,

Mechanism Analysis

This chapter looks at the analytic development of the dynamic equations of the system using the assumed modes method. The results are then compared with those obtained from FEM (Ansys) and via the open loop experiments on the setup.

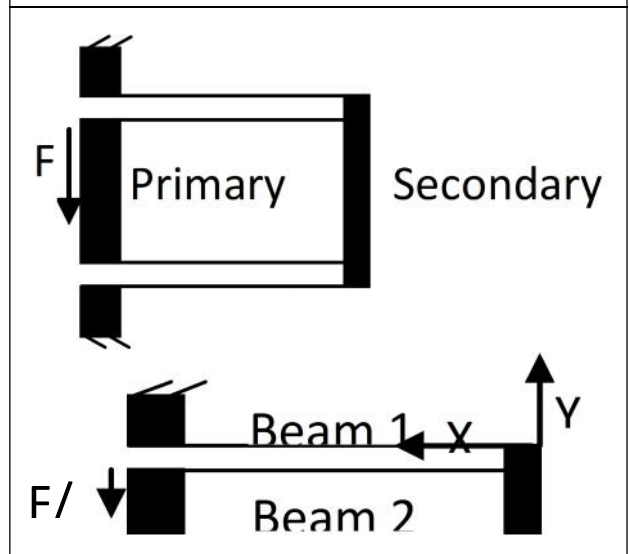
X-Y positioning is achieved using two double parallelogram mechanisms arranged as shown below:

Figure 12: X-Y Positioning Stage with Two Double Parallelogram Flexure Mechanisms



Each stage operates independently of the other. Based on this premise, we can model the X-stage (inside the enclosure) as:

Figure 13: a) X-Stage b) Symmetric Distribution of the Load



By symmetry, we can say that the load is equally shared by the upper and lower halves of the structure. This is depicted in Figure 13.

Dynamic Analysis: Double Flexure Mechanism

Use modal analysis to determine the vibration characteristics (natural frequencies and mode shapes) of a structure or a machine component while it is being designed. It can also serve as a starting point for another, more

Table 1: Modal Analysis Result

Mode	Frequency [Hz]
1	14.3
2	170.19
3	174.75
4	324.53
5	468.33
6	474.22
7	479.39
8	560.71
9	590.08
10	918.42

detailed, dynamic analysis, such as a transient dynamic analysis, a harmonic response analysis, or a spectrum analysis. Summarizing the modal analysis method of analyzing linear mechanical systems and the benefits derived:

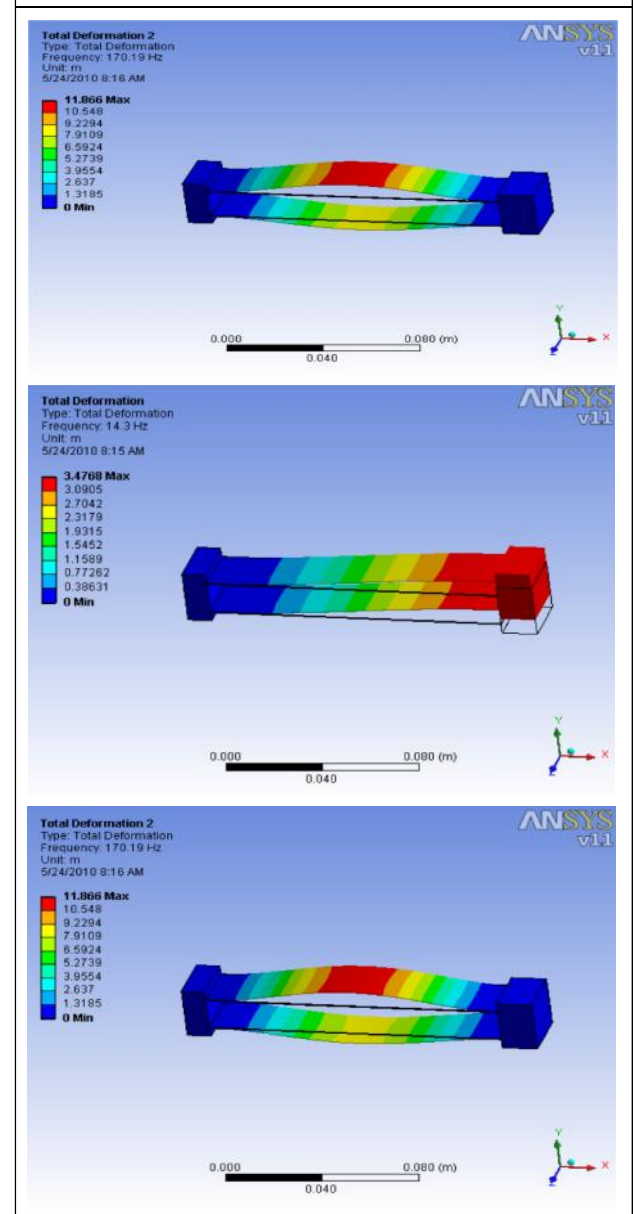
- Solve the undamped eigenvalue problem, which identifies the resonant frequencies and mode shapes (eigenvalues and eigenvectors), useful in themselves for understanding basic motions of the system.
- Use the eigenvectors to uncouple or diagonalizable the original set of coupled equations, allowing the solution of n-uncoupled s dof problems instead of solving a set of n-coupled equations.
- Calculate the contribution of each mode to the overall response. This also allows one to reduce the size of the problem by eliminating modes that cannot be excited and/or modes that have no outputs at the desired dof's. Also, high frequency modes that have little contribution to the system at lower frequencies can be eliminated or approximately accounted for, further reducing the size of the system to be analyzed.
- Write the system matrix, A, by inspection. Assemble the input and output matrices, B and C, using appropriate eigenvector terms. Frequency domain and forced transient response problems can be solved at this point. If complete eigenvectors are available, initial condition transient problems can also be solved. For lightly damped systems, proportional damping can be added, while still allowing the equations to be uncoupled.

ANSYS V11 Workbench is used here to carry out modal analysis of flexural unit used

as basic building blocks of XY planar flexural mechanisms

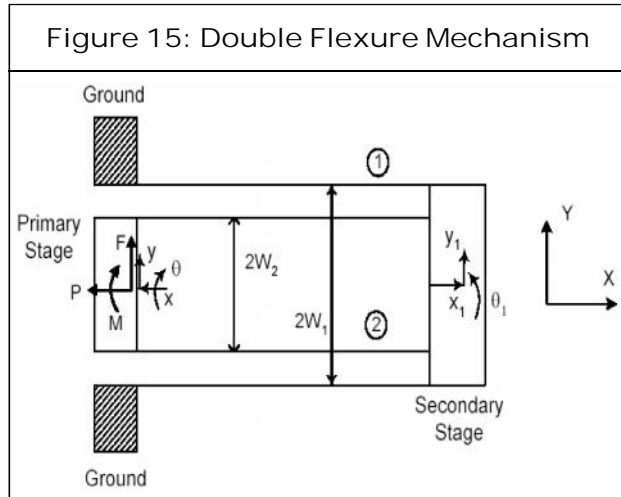
Modal Analysis of Parallelogram Single Flexure

Figure 14: Analysis of Single Flexure Mechanism



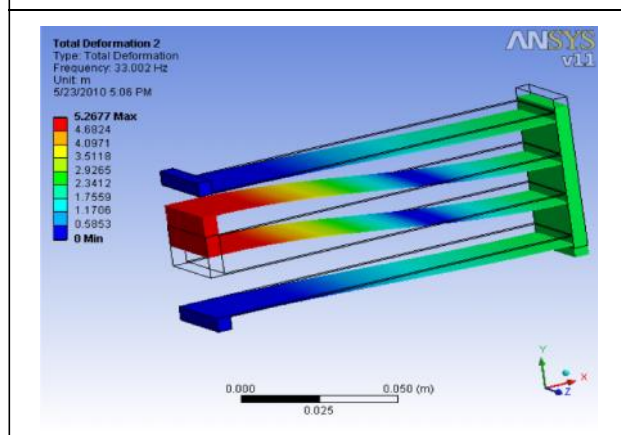
Modal Analysis of Double Flexural Unit

It can be analytically shown that parallelogram flexure offers small resistance to relative



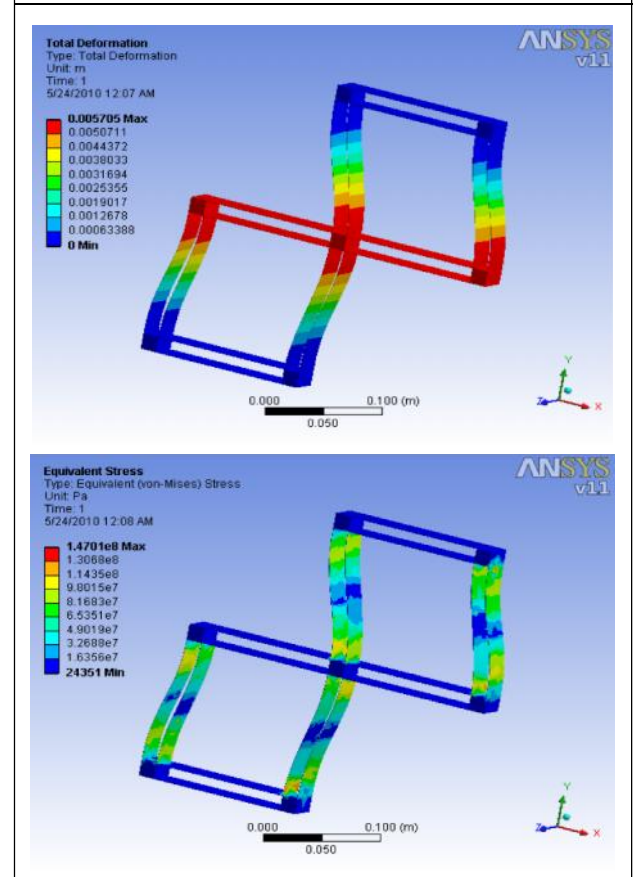
motion in the Y direction but is stiff with respect to relative motion in X and rotation. Hence, it is a much better approximation for single DOF flexure as compared to the simple beam flexure used in the previous case. Two rigid moving platforms are referred to as the primary and secondary platforms. Loads f , m and p are applied at the primary platform. The two parallelograms are treated as identical, except for the beam spacing, w_1 and w_2 . Assumptions similar to the ones stated in the previous section hold here as well. x_1 , y_1 and θ_1 are the absolute displacement coordinates of the secondary stage, and x_2 , y_2 and θ_2 are those of the primary stage, along the directions

Figure 16: Modal Analysis Double Flexure Mechanism



indicated in Figure 15. Force displacement results obtained in the previous section are applied to the constituent parallelograms in the present case. Force equilibrium conditions are obtained by drawing FBDs for each of the platforms.

Figure 17: Modal Analysis of Flexure Mechanism 1



FEM Analysis of Flexural Mechanisms 1 (Static)

The parallelogram flexure unit is a classic design that has been employed in many flexural mechanisms. Due to their finite stiffness, the additional flexure units do not over-constrain the mechanism. This symmetric arrangement should result in several performance improvements. The motion stage yaw should be further reduced to due to the

additional rotational constraints arising from the parallelogram flexures. On the application of an X actuation force, the two sides of the mechanism tend to produce displacements in Y direction that counter each other, and therefore reduce the cross-axis coupling errors. Out of plane stiffness also improves due to better support of the motion stage.

Figure 18: Modal Analysis of Flexural Mechanism 1 (Dynamic)

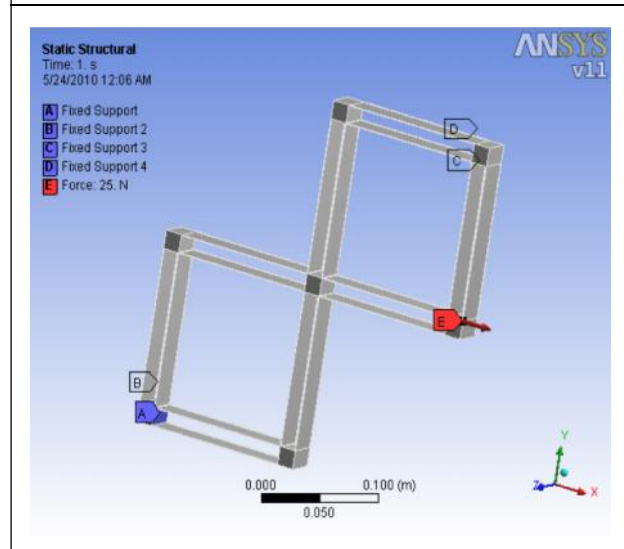


Table 2: Modal Analysis Result

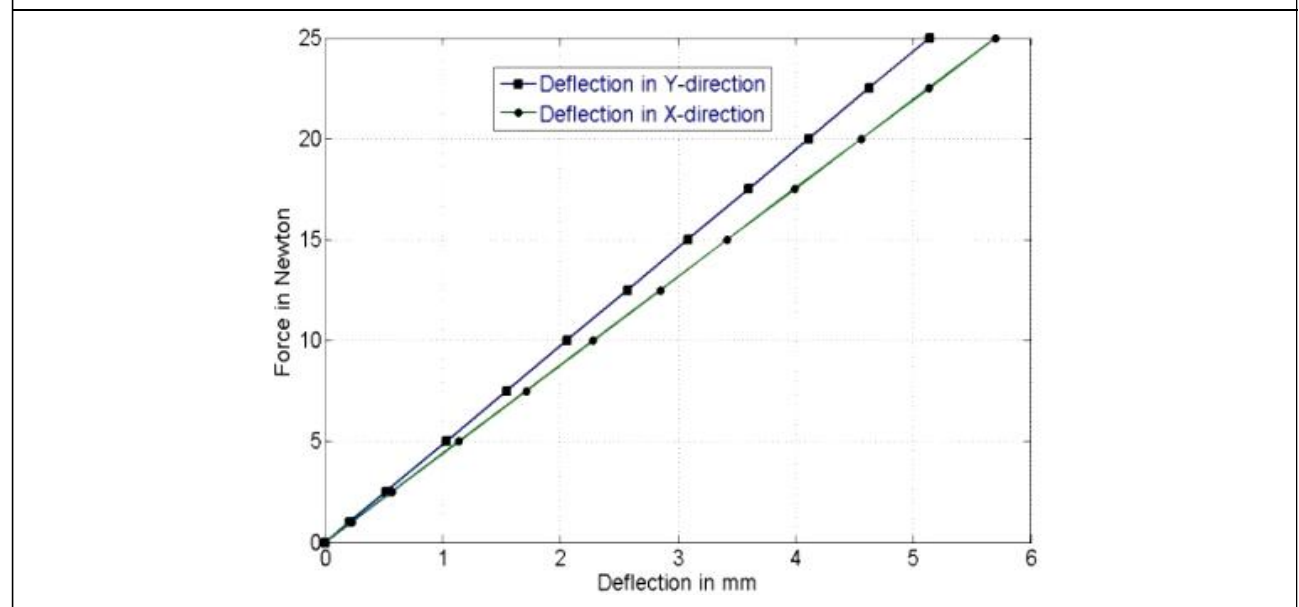
Mode	Frequency [Hz]
1	12.334
2	33.002
3	169.79
4	170.32
5	173.79
6	194.58
7	348.42
8	451.83
9	467.8
10	469.21

Table 3: Modal Analysis Result

Model > Modal > Solution

Mode	Frequency [Hz]
1.	22.562
2.	23.782
3.	216.53
4.	227.99
5.	229.95
6.	240.25
7.	248.25
8.	250.93
9.	253.16
10.	255.48

Figure 19: Plot Force via Deflection



CONCLUSION

There exist many two-axes planer flexural mechanisms that allow for small translations within the plane of the flexure. Most of these designs incorporate a stacked assembly where one linear stage is mounted perpendicular on a second linear stage resulting in a relatively bulky design. Nevertheless, in this arrangement the two axes are entirely decoupled and the actuation of one axis has no effect on the other. Such an assembly is commonly referred to as a 'serial design' in robotics terminology. In some clever serial designs, the above-mentioned stacking is achieved within a plane.

The disadvantage of serial designs is that the actuator for the second stage has to be mounted on the moving member of the first stage. This not only makes the design unnecessarily complex but also limits the system dynamic performance, for example, speed of response. Ideally, it is desirable to mount the actuators for both the axes on ground, i.e., the fixed base.

Furthermore, if one tries to increase the degrees of freedom of a flexural mechanism using the serial approach, the design becomes increasingly cumbersome and bulky. Therefore, instead of taking this path designers usually develop assemblies that are based on closed-chain parallel designs (as opposed to serial designs). In this kind of designs however, parasitic coupling between the degrees of freedom and cross-sensitivity of actuators become performance limiting factors. These two factors are explained in the next section. There are situations where such parallel designs are used, but accuracy is compromised for economy in size. There are other situations where any

degree of errors is unacceptable either at the motion stage itself or at the points of actuator force application. It would be desirable to have mechanisms that have the compactness of parallel designs while axes decoupling and actuator isolation of serial designs.

In this disclosure we shall present a group of flexural mechanisms that are based on parallel elasto-kinematics. It is worthwhile to mention here that the motion of compliant mechanisms is not completely characterized by kinematics; it is strongly dependent on elastic deformations as well. Hence, the study of motion of flexural mechanisms is commonly referred to as elasto-kinematics. Mechanisms presented here make unique use of known flexural units and novel geometric symmetry to minimize or even completely eliminate actuator cross-sensitivity, and parasitic coupling between the two axes.

FUTURE SCOPE

The designs presented in this document are very fundamental and can be used over a wide range of macro, meso or micro scale precision machines where decoupled multiple degrees of freedom are required. Potential applications can be found in optical instruments, Micro and Nano Electro Mechanical Systems, precision metrology, etc. A few specific applications are mentioned here.

High Precision Two or More Axis Motion Stage: In certain high precision microscope that is used for observing the interaction between protein and DNA molecules, the stage that holds the specimen needs to be panned with sub-micron precision. The 2 DOF planer designs presented in this document are ideal candidates for such applications.

Micro-Electro Mechanical (MEM) Motion Stages for Actuators and Bearings: These designs are of very significant consequence to MEMS technology where structures need to be etched on Silicon wafers. Planer designs that provide multiple DOF can have an unprecedented impact on MEMS actuators, bearings and guides.🌀

REFERENCES

1. Awtar S and Slocum A H (2004), "Apparatus Having Motion with Pre-Determined Degree of Freedom", US Patent 6,688,183 B2.
2. Davies P A (2001), "Positioning Mechanism", US Patent 6,193,226.
3. Howell L L (2001), *Compliant Mechanisms*, John Wiley & Sons.
4. Hwa Soo Kim and Young Man Cho (2009), "Design and Modeling of a Novel 3-DOF Precision Micro-Stage", *Mechatronics*, Vol. 19, pp. 598-608.
5. Lobontiu N (2003), *Compliant Mechanisms: Design of Flexure Hinges*, CRC Press.
6. Qing Yao J and Dong P M Ferreira (2007), "Design, Analysis, Fabrication and Testing of a Parallel-Kinematic Micropositioning XY Stage", *International Journal of Machine Tools & Manufacture*, Vol. 47, pp. 946-961.
7. Tian Y, Shirinzadeh B, Zhang D, Liu X and Chetwynd D (2009), "Design and Forward Kinematics of the Compliant Micro-Manipulator with Leaver Mechanisms", *Precision Engineering*, Vol. 33, pp. 466-475.
8. Yangmin Li and Qingsong Xu (2009), "Modeling and Performance Evalutrn of a Flexure-Based XY Parallel Micromanipulator", *Mechanism and Machine Theory*, Vol. 44, pp. 2127-2152.